Experimental test of instability enhanced collisional friction for determining ion loss in two ion species plasmas[a)]

N. Hershkowitz,[1,b)] C.-S. Yip,[1] and G. D. Severn[2]
[1]*Department of Engineering Physics, University of Wisconsin, Madison, Madison, Wisconsin 53706, USA*
[2]*Department of Physics, University of San Diego, San Diego, California 92110, USA*

(Received 29 November 2010; accepted 10 January 2011; published online 7 April 2011)

Recent experiments have shown that ions in weakly collisional plasmas containing two ion species of comparable densities approximately reach a common velocity at the sheath edge equal to the bulk plasma ion sound velocity. A recent theory [S. D. Baalrud, C. C. Hegna, and J. D. Callen, Phys. Rev. Lett. **103**, 205002 (2009)] suggests that this is a consequence of collisional friction between the two ion species enhanced by the two stream instability. The theory finds that the difference in velocities at the sheath edge depends on the relative concentrations of the two ions. The difference in velocities is small, with both species approaching to the bulk sound velocity, when the concentrations are comparable, and is large, with each species reaching its own Bohm velocity, when the relative concentration differences are large. To test these findings, drift velocities of Ar and Xe ions were measured with laser-induced fluorescence in Ar–Xe and He–Xe plasmas and combined with ion acoustic wave and plasma potential data. In addition, electron temperature was varied by a Maxwell demon [K. R. MacKenzie *et al.*, App. Phys. Lett. **18**, 529 (1971)]. The predictions were found to be in excellent agreement with the experimental data. The generalized Bohm criterion in two ion species plasmas is also verified in a wider variety of relative ion concentrations. © *2011 American Institute of Physics*. [doi:10.1063/1.3562574]

I. INTRODUCTION

Langmuir was the first to realize that ions at the sheath edge must have directed velocities greater than their thermal velocity when the ion temperature was much less than the electron temperature.[1] Bohm[2] was the first to argue that the drift velocity needed to be at least the ion sound velocity at the sheath plasma boundary and so this is also called the Bohm velocity. In collisionless and weakly collisional unmagnetized plasmas, ions can be accelerated to the sheath/presheath boundary by presheath electric fields. In collisionless plasmas, ion energy is conserved so cold ions in the bulk plasma only need to fall through a potential difference of $T_e/2e$ (where T_e is measured in units of electronvolts) to reach the Bohm velocity. So if one singly ionized ion species is accelerated to c_s by the presheath electric field, all other singly ionized ion species in the plasma will be accelerated to c_s by the same presheath electric field. Many investigators assumed that all ion species in all weakly collisional plasmas reached their individual Bohm velocity at the sheath-presheath boundary.[3] Combined with the ion species' density, this determined the ion flux at the boundary. Plasma is not collisionless in most laboratory experiments nor in most applications[4] based on low temperature plasma. In weakly collisional plasma in which ion collision lengths λ are much greater than sheath dimensions, ion flow is mobility limited and can be described by $v=\mu E$ where the mobility μ is defined as $\mu=e/(\sigma n_0 v)$, where σ is the ion-neutral collisional cross section and n_0 is the neutral density. Ions must fall through a presheath potential drops greater than $T_e/2e$ to reach the Bohm velocity when collisions are present.[5]

For one ion species, Riemann [6] has shown that mobility limited ion flow in the presheath electric field results in the presheath potential profile can be approximated by

$$\frac{e\Delta\phi}{T_e}\approx\sqrt{\frac{\Delta x}{\lambda}}, \tag{1}$$

when the ion-neutral collision mean free path λ is either a constant or proportional to v . Different ions have different mobilities so the electric field in weakly collisional plasma cannot accelerate more than one ion species to its Bohm velocity. With two *or more ion species and* Maxwellian electrons, Riemann[7] showed that ions satisfy a generalized Bohm criterion

$$1\geq\sum_i (n_i c_{si}^2)/(n_e v_i^2), \tag{2}$$

where all quantities refer to sheath edge values, except the sound speeds, which refer to bulk values. With only two ion species and assuming the equality holds,

$$\frac{n_1 c_{s1}^2}{n_e v_1^2}+\frac{n_2 c_{s2}^2}{n_e v_2^2}=1, \tag{3}$$

and the generalized Bohm velocity can be satisfied by speeds faster or slower than the sound speed for a given ion species. There are two simple solutions: (1) all ions attain the same speed at the sheath edge and (2) each species attains its own Bohm speed. Solution (1) gives a common ion drift velocity v_c at the sheath edge

[a)]Paper CI2 3, Bull. Am. Phys. Soc. **55**, 59 (2010).
[b)]Invited speaker. Electronic mail: hershkowitz@engr.wisc.edu.

$$v_c = \sqrt{\frac{n_1}{n_e}c_{s1}^2 + \frac{n_2}{n_e}c_{s2}^2}. \quad (4)$$

Note that v_c is equal to the ion acoustic speed in a homogeneous plasma with no ion drifts.

Our recent experiments have shown that ions in weakly collisional plasmas containing two ion species of comparable densities very nearly reach a common velocity at the sheath edge within error.[8–10] The common velocity was the bulk system ion sound velocity. In this paper we address the questions: How does the plasma achieve that result? What happens when two ion species do not have comparable masses?

The first clue to answering this question was the observation of significant ion beam-ion beam instability in the presheath.[10] The second clue was the details of the ion flow speeds in the presheath. Laser-induced fluorescence (LIF) data showing the ion flow speeds[11] and the plasma potential profile throughout the presheath in an Ar – Xe plasma with comparable Ar and Xe densities are shown in Fig. 1. These data show the difference in flow speeds throughout the presheath is small and that the difference in rms drift velocity never exceeds 175 ± 50 m/s. The heavy ion (Xe) velocity is faster than the Xe Bohm velocity and the Ar ion beam velocity was slower than the Ar Bohm velocity. The results show that both argon and xenon ions get very close to the ion sound speed in the bulk plasma, with a small but measurable velocity difference.

Baalrud *et al.*[12,13] have recently shown that the ion-ion two stream instability may lead to collisional friction between the two ion species that accelerates the slower species and decelerates the faster one. They show that this effect establishes the solution of Bohm's criterion in two ion species plasmas. The relative flow speed of the two ion species, on account of the instability enhanced, ion-ion collisional friction, was predicted thereby to be limited to a value depending on their thermal velocities, relative densities, and their relative masses. In particular, adopting a fluid theory representation for the instability dispersion relation, they predicted that individual species' velocities equal individual species' Bohm velocities when one species' density was much larger than the other, and that there should be a minimum velocity difference when the ion concentrations are comparable given by

$$\Delta V_c = V_2 - V_1 = \sqrt{\frac{1+\alpha}{2\alpha}}\sqrt{v_{T1}^2 + \alpha v_{T2}^2}, \quad (5)$$

where $\alpha = n_1 M_2/(n_2 M_1)$. However, using a dispersion relation incorporating Maxwellian ion velocity distributions, they found that the minimum velocity differences was given by

$$\Delta V_c = -\frac{3}{2}|v_{T2} - v_{T1}| + \sqrt{\frac{1}{2}\left(v_{T1}^2 + v_{T2}^2 + \frac{n_2 T_1}{n_1 T_2}v_{T1}^2 + \frac{n_1 T_2}{n_2 T_1}v_{T2}^2\right)}. \quad (6)$$

Baalrud *et al.* argued that when the ion masses are very different, the fluid representation will give an accurate approximation of the ion drift velocities, while the kinetic representation assumes a small ion mass differences and is applicable in such cases.

II. EXPERIMENTAL DETAILS

A. Overview

The experiments were carried out in a multidipole confinement device[11] shown schematically in Fig. 2. The base vacuum for most measurements was approximately 0.3 μTorr. Permanent magnet rows (peak fields, 0.1 T) with alternating magnetic polarities, were mounted axially, but not on the chamber end walls. Plasma was produced by electron emission from 21 hot thoriated tungsten filaments (diameter = 0.1 mm, approximately 10 cm long) biased at -60 V with respect to grounded chamber. Electron temperature was measured with 6 mm diameter tungsten disk Langmuir probes. An emissive probe measured the plasma potential profile near a negatively biased plate. The sheath-presheath boundary was identified from the slope change of the emission current versus bias voltage curve. Laser induced fluorescence determined ion flow velocities and ion temperatures. Both Ar^+ and Xe^+ LIF measurements were made. Electron and ion temperatures were varied by changing the bias voltage on a MacKenzie

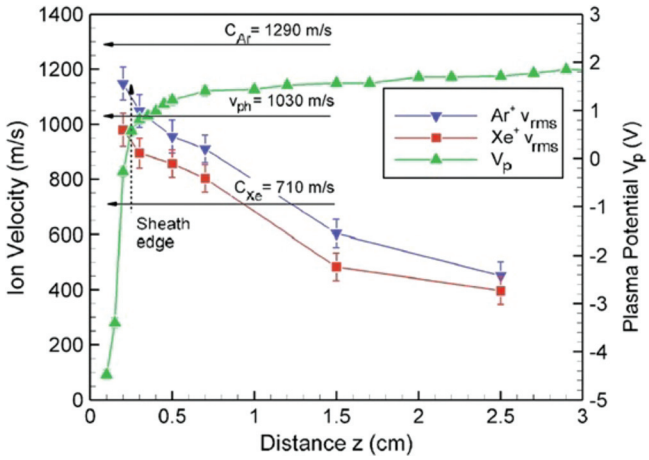

FIG. 1. (Color online) Ar and Xe ion speeds with respect to position relative to the plasma boundary in Ar – Xe plasma.

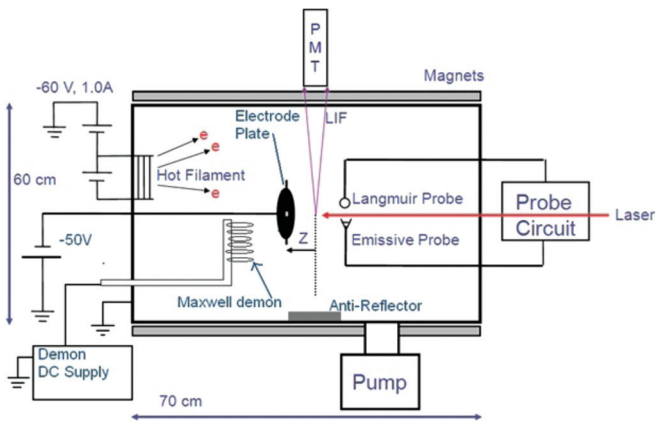

FIG. 2. (Color online) Schematic of the multidipole chamber setup. The beam dump is represented by a gray dot on the plate electrode.

Maxwell demon.[14] The concentration ratio of the two ion species was determined from the phase velocity of ion acoustic waves in the bulk plasma combined with the measured T_e. Ion two stream instabilities were measured with a 1 cm long, 0.025 mm diameter cylindrical probe biased approximately 1–3 V above the plasma potential.

B. LIF

The LIF technique, typically, consists of three procedures, (1) selecting a metastable state in the atom of interest known to be sufficiently populated in plasma discharge to be diagnosed, (2) steering a tunable laser light source through the plasma so as to intersect a region in the plasma to be diagnosed with sufficient power and intensity so that the induced fluorescence produces a measurable photon current or count, and (3) collecting the fluorescence with a photon collector [typically a photomultiplier tube (PMT)], along an optical axis oblique to the incident laser beam, with a collection optics train that sets the spatial resolution of the acquired signal. As seen in Fig. 2, the laser beam was on the cylindrical chamber axis and the PMT was located at a fixed position on the sidewall. The collection optics train also housed a narrowband filter that permitted wavelength filtering so that much of the optical noise was passively reduced. The interference filter had a transmission peak designed to match the wavelength of the most probable decay photon from the excited state of the so-called "LIF scheme," consisting of the metastable state, excited state (between which the transition requires a photon within reach of the tunable laser light source), and the decay state. Our LIF schemes are shown in Fig. 3.

Optical excitation of Ar II metastable and Xe II metastable state ions was accomplished with extended cavity diode lasers[15] capable of providing narrow linewidth tunable laser power; the power, linewidth, and stable detuning (so called because of its association with tuning away from the desired line center) frequency were nominally 20 mW, and 1 MHz, and 5 GHz, respectively. For the transition from the metastable state to the excited state, the LIF scheme for Ar II required a photon wavelength 668.43 nm, and the subsequent decay to the produced a detectable photon with wavelength 442.72 nm. The LIF scheme used in Xe II required a wavelength of 680.57 nm for excitation and 492.15 nm for detection. All wavelengths are given in air. Note also, that unlike Ar II, where the LS (Russell-Saunders) coupling scheme is still valid, Xe II is best described by an intermediate coupling scheme, *jK*, where the total angular momentum of the optically active electron is added to its orbital angular momentum to compose the angular momentum K, set in brackets.[16]

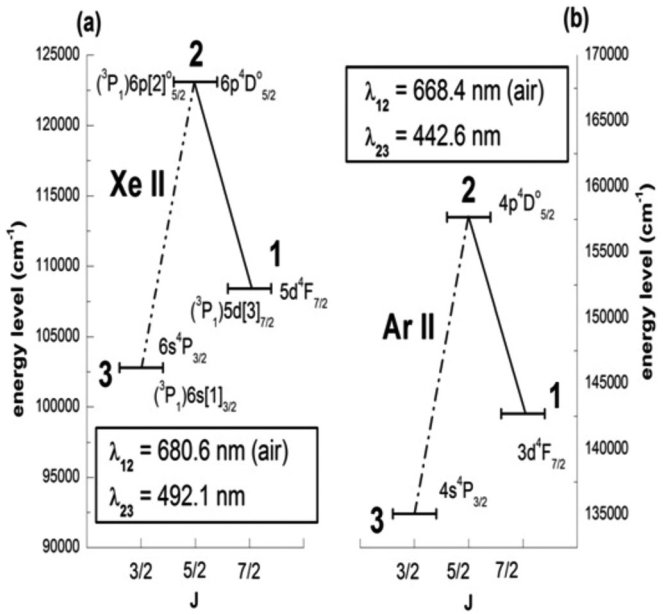

FIG. 3. LIF schemes for both Ar II (a) and Xe II (b). All wavelengths are given for air.

Further noise to signal reduction was accomplished by chopping the indent laser been with a mechanical chopper rotating at 3.1 kHz and using phase sensitive detection of the PMT signal with a lock-in amplifier (Stanford Research Systems SR830). Coarse tuning was aided by use of a Burleigh WA-1000 wavemeter, and fine tuning was accomplished with a programmed voltage ramp of nominally 5 V. Tuning was calibrated using an iodine gas cell interposed between the diode laser and the vacuum chamber. This and an etalon allowed us to verify tuning to within ± 0.001 nm. Still, the noise was such that several single wavelength tuned signal captures were averaged in order to produce the ion velocity distribution functions (IVDFs) used to calculate ion velocity moments.

These were calculated as follows. The IVDF, $f(v_z, z)$, was obtained from the LIF signal, $f(\Delta f_d,z)$, a function of the detuning frequency, using the first order Doppler shift,

$$v_z = \frac{c\Delta f_d}{f_o + \Delta f_d} \approx \frac{c\Delta f_d}{f_o} = \lambda_o \Delta f_d, \tag{7}$$

where v_z is the ion velocity, c is the speed of light, λ_o is the excitation wavelength at the line center, f_o is the excitation frequency at the line center, and Δf_d is the detuning from the line center. The first moment of the IVDF, the flow speed,

$$\langle v_z \rangle = \int_{-\infty}^{\infty} v_z f(v_z, z) dv_z \Big/ \int_{-\infty}^{\infty} f(v_z, z) dv_z \tag{8}$$

was used to compare with theory. It is assumed that the ion metastable state is in thermal equilibrium with the ground state ion.

C. Emissive probe technique

Plasma potential is measured by an emissive probe with the inflection point technique.[17] One finds the plasma potential by graphing inflection points of I-V traces and extrapolates them to zero emission. Furthermore, within the sheath edge, the inflection points become more positive with increased emission, while in the bulk this effect is reversed,[18] indicating the spatial location at which at which space charge begins and the quasineutral plasma ends. Thus one can identify the sheath edge in a two species plasma by observing the point where inflection point changes from increasing with emission to decreasing with emission. Figure 4 shows an example of such change in the slope of infection

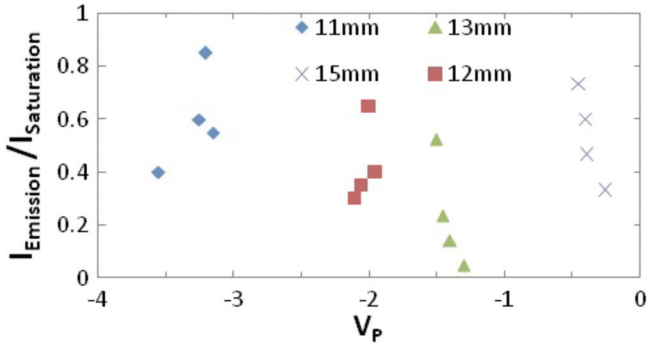

FIG. 4. (Color online) Emission current of the inflection points are plotted against the potential at which they occur at different positions from the plate electrode.

points, the plasma shown in this figure had a sheath thickness between 12 and 13 mm. The corresponding plasma potential profile is shown in Fig. 5.

D. Ion acoustic wave diagnostics (continuous wave)

Ion acoustic waves (IAWs) were launched by a 7 cm diameter circular grid with a function generator, and were detected with a 0.25 in. Langmuir probe biased at −67 V to collect ion saturation current. A Boxcar averager[19] was employed to do time sampling and averaging. A family of spatial profiles of the signal amplitude versus launcher-detector separation were created by systematically incrementing the trigger delay with the result that the phase velocity of the IAWs could be easily measured. The relative concentrations of the ions were inferred[20] from the phase velocity in the two ion species plasma.

E. Mackenzie's Maxwell demon

The first version of a plasma Maxwell demon, implemented by Mackenzie *et al.*[14] consisted of a wire mesh or grid immersed in the plasma. When a positive bias is applied to the grid, cold electrons are collected at the grid while the hot electrons with a sufficiently great angular momentum are not trapped and remain in the bulk plasma. This results in an increase in the plasma electron temperature. The system is not isolated in any important sense, and the surroundings also warm up and no net entropy reduction occurs. However,

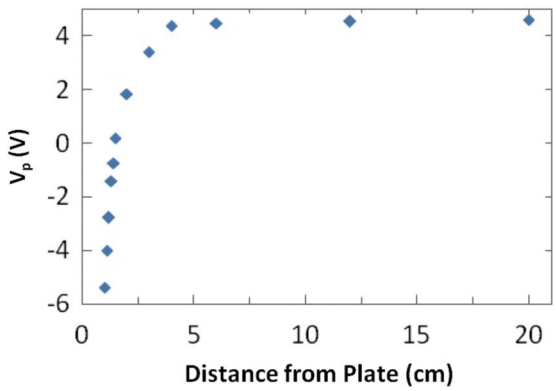

FIG. 5. (Color online) Plasma potential profile obtained by the emissive probe in the vicinity of the boundary plate.

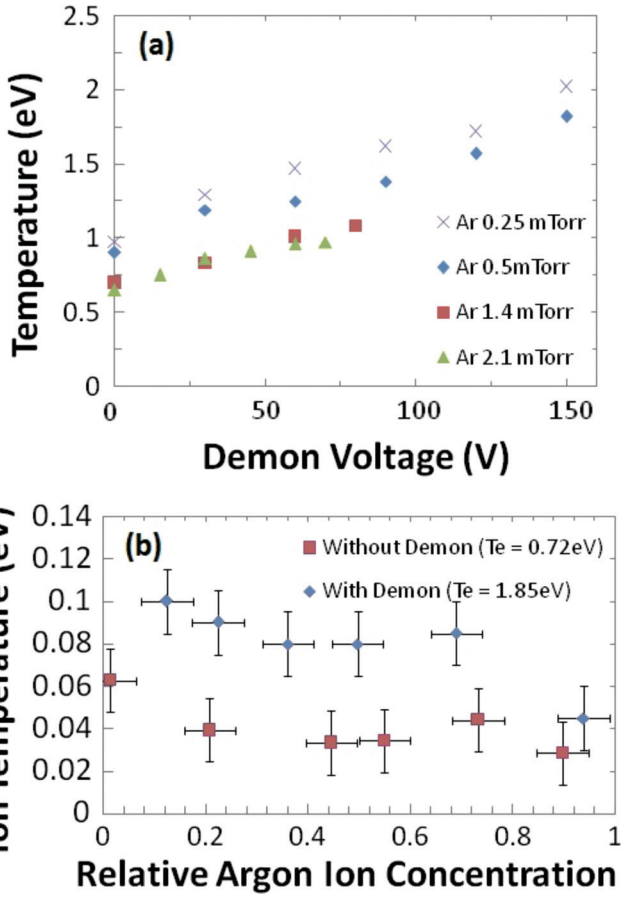

FIG. 6. (Color online) Electron temperature (a) in argon plasmas of different neutral pressure plotted against demon voltage. Higher neutral pressure results in a smaller range of data points due to an instability introduced by the demon. Xenon ion temperature (b) at sheath edge plotted against relative argon ion concentration measured by ion acoustic wave diagnostics. Diamonds are ion temperatures with the demon turned on and squares are those with demon turned off.

the device can be used to control the electron temperature in a plasma discharge, as in the experiments reported here.

Mackenzie's original design was a 60 m×60 cm grid with a total of 400 0.03 mm tungsten wires. Our Maxwell demon consists of approximately 3 m of 0.025 mm tungsten wires spot welded on a shaft. The shaft was electrically isolated from the chamber (and the plasma) and positively biased to absorb cold electrons, thus resulting in plasma heating.

As shown in Fig. 6, our demon was found to be an effective means to increase electron temperature despite its radically different design compared with that of Mackenzie's demon. Wave and demon ion velocity measurements in a xenon plasma indicated that its electron temperature was nearly doubled from 0.89 to 1.71 eV using our demon. The ion acoustic phase velocity measurement (1110 ± 70 m/s) agreed within error with ion phase velocity predicted from T_e measured by the Langmuir probe (1.71 eV gives 1120 ± 70 m/s). Futhermore, the measured ion flow speed at the sheath edge (1070 ± 70 m/s) agreed within error with that predicted by the Bohm criterion given this measured T_e, as shown in Fig. 7. Note that as the demon increases the electron temperature of the plasma the ion temperature also increases, as shown in Fig. 6.

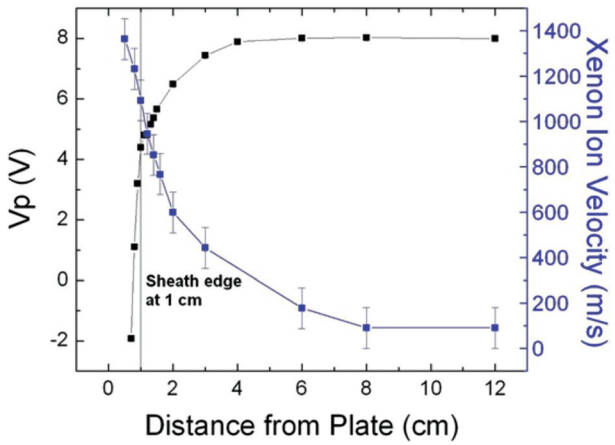

FIG. 7. (Color online) Plasma potential and ion velocity of a xenon plasma with the temperature raised by the demon, plotted against the distance from the electrode plate. Black squares with increasing value with distance is the plasma potential and blue ones with decreasing value over distance is ion velocity.

F. Penning ionization

Measurements of plasma with helium is complicated by Penning ionization[21] of the other neutrals by the helium neutral metastables. This results in relative ion concentrations of the other species to helium being much higher than their relative neutral concentrations. The phase velocities of ion acoustic waves measured in the bulk plasmas were used to determine the relative ion concentrations. Results for xenon–helium plasma are shown in Fig. 8. Note that when the xenon neutral concentration is approximately 10%, its fraction ion concentration is above 80%. Similar results to a lesser degree were observed in xenon–argon plasmas, where the argon metastables ionized xenon neutrals, as shown in Fig. 9. In this case an approximate xenon neutral concentration of 40% results in an approximate xenon ion concentration of nearly 80%.

III. RESULTS

A. Instability measurements

The amplitude, normalized by plasma density, of the instability observed in xenon–argon plasmas at the sheath edge is graphed with respect to the relative argon ion concentration in Fig. 10. The presence of the instability when only one species was present suggests the presence of unidentified impurity ions. The base vacuum for this set of measurements was only 1 μTorr. Identification as a two-stream instability was determined by its dependence on both the relative ion concentrations, and by its spatial profile, measured relative to the boundary plate, as shown in Fig. 11. The dependence on both, particularly that it peaks near the sheath edge, is crucial in showing that this instability is the two stream instability. It shows the instability requires both the existence of two ions and drift velocity differences that arise from acceleration through the presheath. Similar instability was observed in xenon–helium plasmas, with its amplitude graphed with respect to the relative ion concentrations in Fig. 12 and with respect to distance from the plate in Fig. 13. A similar dependence of the relative ion concentration and distance can be observed. However, in a xenon–helium plasma instability was only observed when helium ions are the majority, the reason for such observation is unknown.

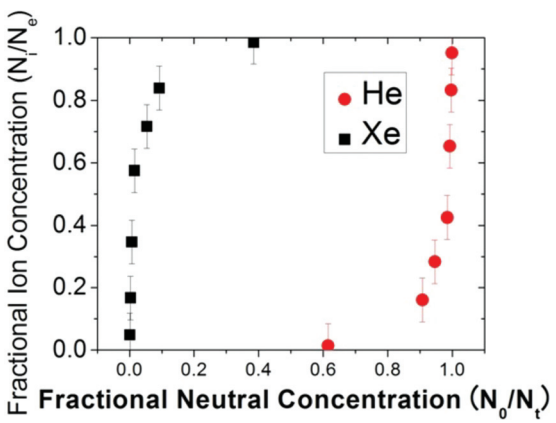

FIG. 8. (Color online) Relative helium ion concentration in red circles and relative xenon ion concentration in black squares are plotted against their respective relative neutral concentration.

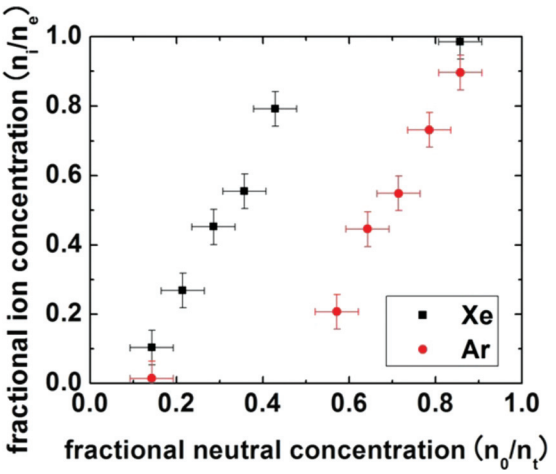

FIG. 9. (Color online) Relative argon ion concentration in red circles and relative xenon ion concentration in black squares are plotted against their respective relative neutral concentration.

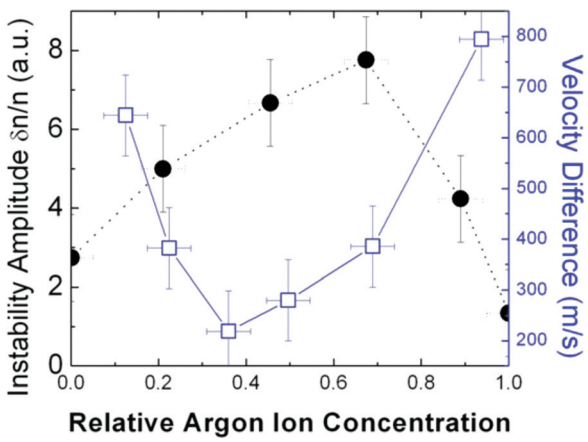

FIG. 10. (Color online) Amplitude of ion-ion stream instability at 1 cm from the plate electrode in solid circles and ion velocity difference in hallow squares plotted against the relative argon concentration of xenon–argon plasmas at $T_e = 1.78$ eV.

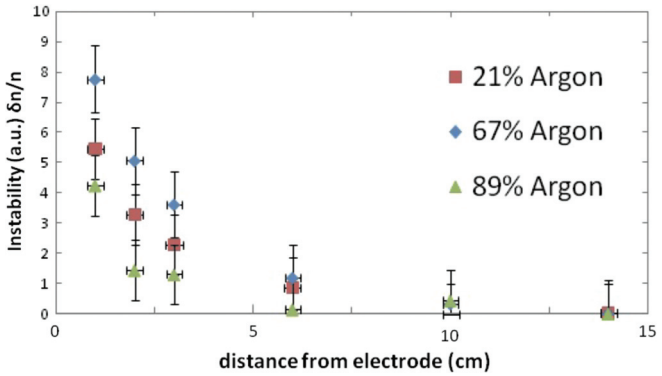

FIG. 11. (Color online) Relative amplitude of ion-ion stream instability measured in 1.78 eV argon–xenon plasmas plotted with the distance from the electrode.

B. LIF measurements

Experimental measurements of argon and xenon ions drift velocity at the sheath edge of a 0.7 mTorr plasma are compared with the theory curves based on the predictions of the kinetic version of the theory of Baalrud *et al.*[12] in Fig. 14. The theory curves corresponds to predicted Ar II and Xe II sheath edge flow speeds, and the data are first moments of the measured IVDFs. It is clear that there is excellent agreement with the experimental measurements in which ion temperatures[9] for both species varied from 0.04 to 0.05 eV. Notice that as the system sound velocity is close to the lighter species' sound velocity as the lighter ions become the majority of the plasma, the system sound velocity also agrees with the argon species' measured drift velocity. This effect was also observed in experiments with different electron temperatures and ion masses.

Experimental measurements at higher electron and ion temperatures and lower neutral argon partial pressures ranging from 0.07 to 0.13 mTorr of the xenon and argon ion drift velocities at the sheath edge are compared with the predictions of Baalrud *et al.*[12] The electron temperature, controlled by the maxwell demon, was 1.78 ± 0.03 eV, and the xenon ion temperature varied from 0.06 to 0.1 eV as shown in Fig. 6. Fitting the theory curves of the kinetic version of Baalrud *et al.*'s

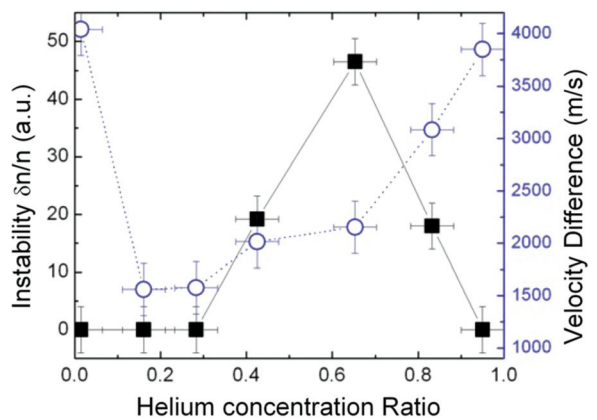

FIG. 12. (Color online) Amplitude of ion-ion Stream instability at 1 cm from the plate electrode in solid squares and ion velocity difference in hallow circles plotted against the relative argon concentration of xenon–helium plasma.

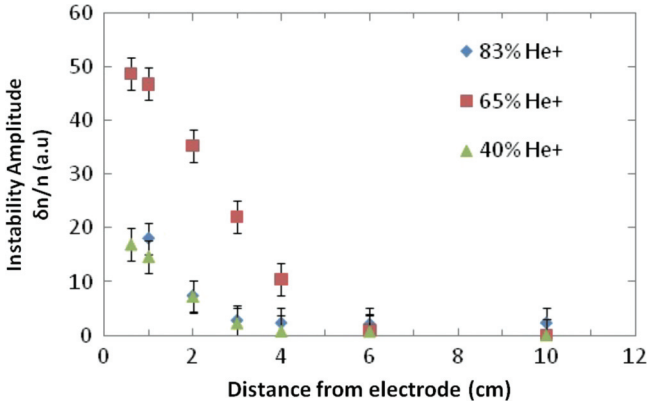

FIG. 13. (Color online) Relative amplitude of ion-ion stream instability measured in helium–xenon plasma of different relative helium concentration plotted against the distance from the plate electrode. A good part of the 85% helium ions and 40% helium ions data overlapped until 1 cm from the plate and therefore not visible in the graph.

theory with these parameters to the experimental data is shown in Fig. 15, which demonstrates excellent agreement between the experimental measurements and the theoretical predictions. Note that the argon ions are also determined to be close to the system sound velocity as they become the majority ion of the plasma.

To test Baalrud's claim that the fluid approximation applies well with large ion mass differences, xenon ion velocities at the sheath edge of XeHe plasmas were measured, and the helium ion velocities at the sheath edge were calculated given the measured xenon ion velocity, and by assuming that generalized Bohm criterion holds. With a variation of T_e from 1.2 to 0.6 eV and T_i from 0.04 to 0.12 eV, as shown in Fig. 16, all velocities are effectively normalized to their own Bohm speeds (i.e., they are normalized to $\sqrt{T_e}$) and are compared to the fluid theory prediction in Fig. 17. The theoretical curve is fit with $T_i = 0.08$ eV and also demonstrates very good agreement between theory and experiment.

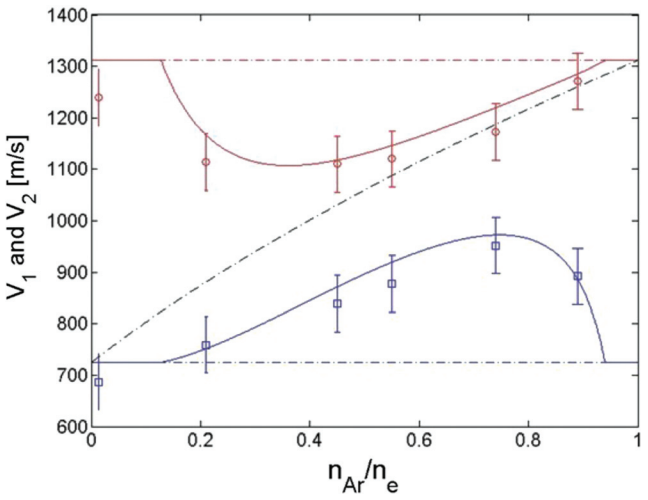

FIG. 14. (Color online) Xenon ion drift velocity at sheath edge in circles and argon ion drift velocity at sheath edge in squares are plotted against the relative argon ion concentration in $T_e = 0.68$ eV plasmas. Blue (lower) and red (upper) solid lines represents theoretical prediction of velocities of xenon and argon ions, respectively, each species' own Bohm's velocity and the common sound velocity are represented by dashed-dotted lines.

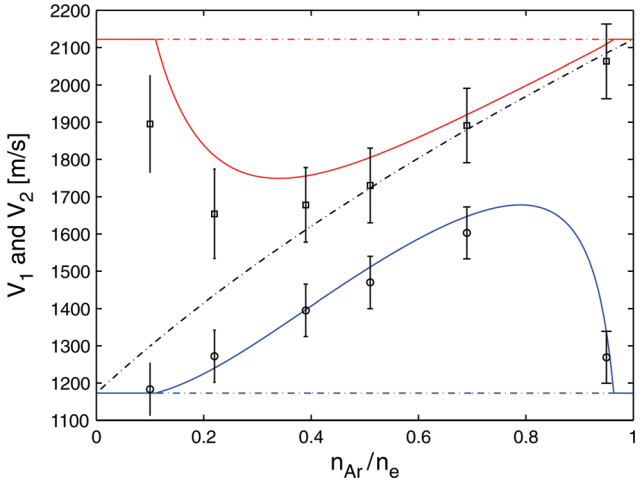

FIG. 15. (Color online) **X**enon ion drift velocity at sheath edge in circles and argon ion drift velocity at sheath edge in squares are plotted against the relative argon ion concentration in T_e=1.78 eV plasmas. Blue (lower) and red (upper) solid lines represents theoretical prediction of velocities of xenon and argon ions, respectively, each species' own Bohm's velocity and the common sound velocity are represented by dashed-dotted lines.

IV. SUMMARY

The generalized Bohm criterion in a two ion species plasma has been verified for Ar–Xe plasmas for a range of relative concentrations running from less than 5% argon ions to approximately 90% argon ions. The effect of Penning ionization both by helium neutrals and by argon neutrals on the heavier species resulted in relative ion concentrations that were very different than the relative neutral concentrations. LIF data of the argon and xenon drift velocities at the sheath edge in argon-xenon plasmas are in excellent agreement with the kinetic version of Baalrud *et al.*'s theory based on ion-ion streaming instability-enhanced collisional friction, which Baalrud *et al*. claimed to be applicable when ion mass ratio is in the order of magnitude of 1. Xenon LIF measurements in xenon–helium plasmas for which ion mass differs by a factor of 33, agree well with the fluid version of the theory, which Baalrud *et al*. claimed to be applicable for ion mass differences greater than a factor of 10. LIF measurement of in argon–xenon plasmas, for which the use of Maxwell demon increased T_e by a factor of 2.5, were also in excellent agreement with the kinetic version of the collisional friction theory. It was also observed that in all cases, the lighter species' drift velocity tracks with the system sound velocity once the lighter species becomes the majority of the plasma ions. In general, ions do not fall out of plasmas with their individual Bohm velocities except when their relative concentrations are either very large or very small.

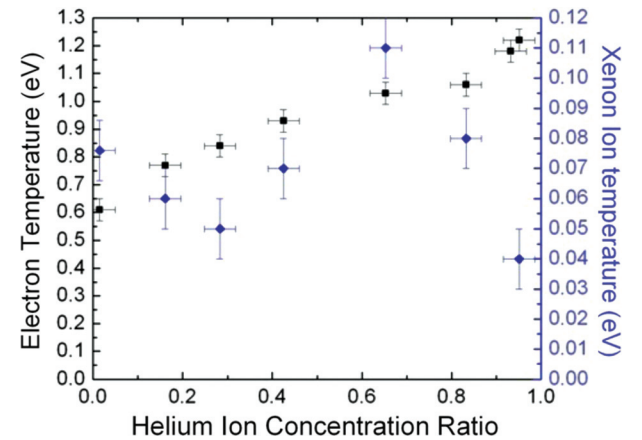

FIG. 16. (Color online) Electron and xenon ion temperature graphed against helium ion concentration ratio. Xenon ion temperatures are represented by blue diamonds and electron temperatures are represented by black squares.

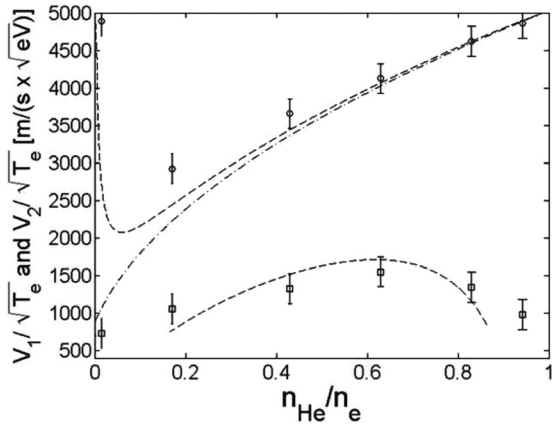

FIG. 17. Xenon ion drift velocity at sheath edge in squares and helium ion drift velocity at sheath edge in circles are plotted against the relative helium ion concentration. Dashed lines represents theoretical prediction of velocities of xenon and helium ions, respectively, the common sound velocity are represented by dashed-dotted lines.

ACKNOWLEDGMENTS

We acknowledge helpful discussions with Dr. Scott Baalrud. This work is supported by U.S. DOE under Grant Nos. DE-FG02-97ER54437, DE-FG02-03ER54728, DE-FG02-06ER54845, DE-AC52-07NA27344, DE-FG02-05ER54809, and DE-FG02-07ER54917, and by the National Science Foundation under the Grant Nos. CBET-0903832 and CBET-0903783.

[1]L. Tonks and I. Langmuir, Phys. Rev. **34**, 876 (1929);I. Langmuir, J. Franklin Inst. **214**, 275 (1932).
[2]D. Bohm, *The Characteristics of Electrical Discharges in Magnetic Fields* (McGraw-Hill, New York, 1949), Chap. 3.
[3]R. N. Franklin, J. Phys. D **33**, 3186 (2000).
[4]M. Lieberman and A. Lichtenberg, *Principles of Plasma Discharges and Materials Processing* (Wiley, New Jersey, 2005).
[5]J. T. Scheuer and G. A. Emmert, Phys. Fluids **31**, 1748 (1988).
[6]K. U. Riemann, Phys. Plasmas **4**, 4158 (1997).
[7]K.-U. Riemann, IEEE Trans. Plasma Sci. **23**, 709 (1995).
[8]D. Lee, N. Hershkowitz, and G. Severn, Appl. Phys. Lett. **91**, 041505 (2007).
[9]C. S. Yip, N. Hershkowitz and G. Severn. Phys. Rev. Lett. **104**, 225003 (2010).
[10]N. Hershkowitz, X. E. Ko, and A. Hala, IEEE Trans. Plasma Sci. **33**, 631 (2005).
[11]D. Lee, N. Hershkowitz, and G. Severn, Appl. Phys. Lett. **91**, 041505 (2007).
[12]S. Baalrud and C. Hegna, University of Wisconsin Report No. UW-CPTC 10-2, 2010.
[13]S. Baalrud, J. Callen, and C. Hegna, Phys. Rev. Lett. **103**, 205002, (2009).
[14]K. R. MacKenzie, R. J. Taylor, D. Cohn, E. Ault, and H. Ikezi, App. Phys. Lett. **18**, 529 (1971).
[15]I. Hildebrandt, R. Knispel, and J. Sacher, Tech. Mess. **68**, 374 (2001).
[16]J. E. Hansen and W. Persson, Phys. Scr. **36**, 602 (1987).
[17]J. R. Smith, N. Hershkowitz, and P. Coakley, Rev. Sci. Instrum. **50**, 210 (1979).
[18]X. Wang and N. Hershkowitz, Rev. Sci. Instrum. **77**, 043507 (2006).
[19]L. Oksuz, D. Lee, and N. Hershkowitz, Plasma Sources Sci. Technol. **17**, 015012 (2008).
[20]A. Hala and N. Hershkowitz, Rev. Sci. Instrum. **72**, 2279 (2001).
[21]M. J. Druyvesteyn and F. M. Penning, Rev. Mod. Phys. **12** 87 (1940).